Original Article

JCBFM

Journal of Cerebral Blood Flow & Metabolism
1–15

DOI: 10.1177/0271678X251399014
journals.sagepub.com/home/jcbfm
Sage

DPSCs-Exos promote OPCs differentiation and white matter repair via Myl9-mediated PRMT5 nucleation after ischemic stroke

Weihong Du[1]*, Panpan Geng[1]*, Zheng Lian[2], Yanyun Sun[3], Yong Zhou[4], Chun Guo[5] and Xinchun Jin[1]

Abstract

Ischemic stroke often leads to white matter damage due to impaired oligodendrocyte precursor cells (OPCs) differentiation, hindering post-stroke recovery. While dental pulp stem cells-derived exosomes (DPSCs-Exos) have shown promise in stroke recovery, the underlying mechanisms remain unclear. Toward this aim, we investigated the therapeutic potential of DPSCs-Exos for promoting OPCs differentiation and white matter repair after ischemic stroke using in vivo (middle cerebral artery occlusion, MCAO) and in vitro (oxygen-glucose deprivation/reoxygenation, OGD/R) models. Intracerebroventricular DPSCs-Exos were administered on days 1, 3, and 5 post-MCAO, with functional (sensory-motor and cognitive), morphological, and biochemical assessments performed at 7, 14, and 28 days. Our results demonstrated that DPSC-Exos treatment significantly improved functional outcomes, promoted OPCs proliferation and differentiation, and facilitated white matter repair. Mechanistically, DPSC-Exos-mediated OPCs differentiation involves protein arginine methyltransferase 5 (PRMT5) and inhibitor of differentiation 2 (ID2). Specifically, exosomal myosin regulatory light polypeptide 9 (Myl9) interacts with PRMT5 in OPCs, driving PRMT5 nucleation, subsequent CpG island methylation, and ID2 downregulation, ultimately leading to OPCs differentiation into oligodendrocytes (OLs). These findings identify a novel mechanism by which DPSC-Exos promote white matter repair and suggest their potential as a therapeutic strategy for ischemic stroke.

Keywords

DPSCs-Exos, ischemic stroke, OPCs differentiation, PRMT5, white matter

Received 13 April 2025; Revised 29 August 2025; Accepted 25 September 2025

Introduction

White matter, with its comparatively limited collateral blood circulation, exhibits heightened vulnerability to ischemia.[1] White matter damage constitutes approximately half of the infarct volume and plays a significant role in neurological impairment.[2,3] Emerging evidence suggests a strong correlation between post-stroke white matter repair and improved neurological recovery.[4,5] Remodeling of cerebral white matter injury relies on the proliferation, migration, and differentiation of oligodendrocyte precursor cells (OPCs) into mature oligodendrocytes (OLs) that enwrap axons to form myelin sheaths.[6,7] However, the adult brain's self-repair capacity after stroke is limited, with only a small fraction of OPCs differentiating and maturing into OLs, resulting in incomplete functional recovery.[6,8]

[1]Department of Histology and Embryology, School of Basic Medical Sciences, Advanced Innovation Center for Human Brain Protection, Capital Medical University, Beijing, China
[2]Department of Biochemistry and Molecular Biology, Capital Medical University, Beijing, China
[3]Institute of Neuroscience, The Second Affiliated Hospital of Soochow University, Suzhou, China
[4]Beijing SH Biotech Corporation, Beijing, China
[5]School of Biosciences, University of Sheffield, Sheffield, UK

*These authors contributed equally to this work.

Corresponding author:
Xinchun Jin, School of Basic Medical Sciences, Capital Medical University, 10 Xitoutiao Youanmenwai, Beijing 100069, China.
Email: xinchunjin@gmail.com

Therefore, investigating the mechanisms and identifying strategies to promote OPCs differentiation after ischemic stroke is crucial.

Dental pulp stem cells (DPSCs) transplantation has been a promising strategy for restoring neurological function after stroke.[9–11] Exosomes (Exos), compared with stem cells, offer advantages in crossing the blood-brain barrier (BBB) and ease of storage and transport.[12] Consequently, exploring the effects and mechanisms of DPSCs-derived exosomes (DPSCs-Exos) on promoting OPCs differentiation and white matter repair is of paramount importance.

The inhibitor of differentiation 2 (ID2) is mainly expressed in OL lineage cells, and ID2 in the nucleus can negatively regulate OLs development and maturation.[13–16] ID2 overexpression inhibits OPCs differentiation into OLs,[17] while ID2 knockdown has an opposite effect.[14] OPCs differentiation is increased when there is less ID2 in the nucleus.[6] Therefore, either limiting ID2 in the cytoplasm[18] or decreasing its expression in the nucleus[19] is a promising strategy to promote OPCs differentiation. It has been reported that ID family protein expression is epigenetically regulated by DNA methylation,[14] and ID2 expression is specifically modulated by protein arginine methyltransferase 5 (PRMT5) through methylation of CpG islands within the *ID2* gene during glial cell differentiation.[19] Notably, PRMT5 is crucial for OPCs differentiation and myelin formation,[20] and its subcellular distribution correlates with OPCs differentiation status.[21] However, it is unclear whether DPSCs-Exos promote OPCs differentiation by affecting the expression and subcellular distribution of PRMT5 within the OL lineage, thereby inhibiting ID2 expression. It has been shown that myosin regulatory light polypeptide 9 (Myl9), an important cytoskeletal component, acts as a regulator of myelin formation.[22] Given that DPSCs-Exos contain a variety of proteins, it is pertinent to investigate whether they can regulate PRMT5 subcellular distribution via Myl9, and consequently promote OPCs differentiation. This potential mechanism warrants further investigation.

In the current study, we investigated the effects of DPSCs-Exos on OPCs differentiation and white matter repair, along with the underlying mechanism using in vitro and in vivo models.

Materials and methods

Animals

The wild-type male C57BL/6J mice (8–10 weeks old) in this study were purchased from the Charles River (Beijing, China). The PRMT5 floxed line was purchased from the Shanghai Model Organisms Center (Shanghai, China), PDGFRα-CreERT2 mouse line from the Li Laboratory. All animal experiments used were approved by the Animal Experiments and Experimental Animal Welfare Committee of Capital Medical University (AEEI-2023-020) and strictly followed the National Institutes of Health (NIH) guidelines for the use and care of laboratory animals. This study is reported according to the ARRIVE guidelines. The mice were kept in the Laboratory Animal Department of Capital Medical University for 12 h on a light/dark cycle and were given free water and a standard laboratory diet. Animals were randomly assigned to groups by the study director who was blinded to all biometric data. Investigators were blinded to group allocation when performing all data collection. No animals were excluded for failure to achieve the predicted phenotypes.

Generation of tamoxifen-inducible OPCs-targeted PRMT5 loss of function mice (PDGFRα-CreERT2; PRMT5$^{flox/flox}$)

To induce PRMT5 deletion, mice with PRMT5$^{f/f}$ genotype were bred with PDGFRα-CreERT2 mice to obtain PRMT5$^{f/f}$: PDGFRα-CreERT2 mice (PRMT5^{iOPCKO}). OPCs specific deletion PRMT5 was induced by tamoxifen (T5648, Sigma, USA) (dissolved in corn oil at 20 mg/mL), and intraperitoneally injected at 100 mg/kg for 5 days. PRMT5$^{f/f}$ mice receiving tamoxifen injection were used as controls.

Transient middle cerebral artery occlusion mouse model

Middle cerebral artery occlusion (MCAO) was performed as previously described.[23] In brief, the ischemia model was induced in 8–10 weeks old adult mice. Mice were anesthetized with isoflurane and kept supine on a heating plate at a constant temperature of 37°C ± 0.5°C throughout. After 60 min of MCAO, reperfusion was initiated by removing the suture.

Isolation, culture, and identification of dental pulp stem cells (DPSCs)

DPSCs, which were donated by Beijing SH Biotech Corporation, were isolated and identified as described by previously published methods.[24] Briefly, the crowns of human impacted third molars were removed, pulp tissue was retained, and α-modified Eagle medium (α-MEM; Gibco; Grand Island) was immersed for 5 min and rinsed five times with PBS. Collagenase and dispase were added to the clipped pulp and digested on a shaker at a constant temperature for 60 min. α-MEM supplemented with 10% fetal bovine serum (FBS; Thermo Fisher Scientific) was used for incubation at 37 °C in 5% CO_2. Cells were used after 4 to 6 passages and the conditioned medium was changed to serum-free medium. Cells were identified by immunostaining using the DPSCs marker CD73 (Santa

Cruz, USA) (Figure S1(A) and (B)). Flow cytometry analysis demonstrated that DPSCs express CD105, CD73, and CD90, but do not express CD11b, consistent with the characteristics of DPSCs (FigureS1(C)-(F)).

Isolation, identification, and labeling of DPSCs-Exos

DPSCs-Exos were extracted from pulp stem cell culture supernatants by continuous centrifugation and ultracentrifugation, as previously described by Zhang et al.[25] DPSCs-Exos were diluted with PBS and dropped on a copper-coated palladium grid, stained with phosphotungstic acid, and observed and captured by transmission electron microscopy (TEM) (H-7650, Hitachi, Japan). The particle size distribution and concentration of DPSCs-Exos were assessed according to nanoparticle tracking analysis (NTA, Brookhaven, NY). Inject the moderately diluted DPSCs-Exos into the sample chamber and place it in the Zeta potential analyzer to calculate the Zeta potential value (Figure S1(G)–(I)).

Protein denaturation was performed after protein concentration in DPSCs-Exos was measured by the BCA Protein Assay Kit (Beyotime, China). SDS-PAGE was performed for gel electrophoresis and electrotransfer to solid-phase PVDF membranes (Millipore, USA), blocked by 5% skimmed milk for 2 h at room temperature, and the primary antibody was incubated at 4°C overnight. The expression of exosomal markers CD63 and CD81 (Santa Cruz, USA) and DPSC marker CD73 (Santa Cruz, USA) were detected (Figure S1(J)).

In the DPSCs-Exos uptake test, 2 μL PKH26 fluorescent dye (MINI26, Sigma, USA) was incubated with 500 μL Dilution C for 5 min at room temperature, then 200 μL exosome-removing FBS was added. The labeled DPSCs-Exos were washed with PBS and subsequently centrifuged at 100,000*g* for 70 min at 4 °C, and finally suspended in PBS. OPCs cultured in PKH26-labeled DPSCs-Exos medium, with NG2 staining indicating that DPSCs-Exos could be uptaken by OPCs (Figure S3(C)).

DPSCs-Exos delivery system

DPSCs-Exos (2.5×10^9/8 μL/day, dissolved in PBS) were intra-ventricle infused through a guide cannula 1, 3, and 5 days after MCAO.

Behavioral tests

Neurological scores

The neurological scores (0–7) were used to dynamically assess neurological deficits at 1, 3, 7, and 14 days after reperfusion with higher scores indicating more severe neurological deficits.[26]

Corner test

Corner test was performed as previously reported.[27] Mice were put between two boards with a 30° angle (to simulate a corner), and the direction in which the mice turned (left or right) after placing the corner was observed and recorded 10 times. In theory, the turning of sham group mice was random, while the turning of MCAO mice tended to be on the nonischemic side.

Foot-fault test

Foot fault was tested as previously described.[28] Each mouse was placed on a steel gridded floor (35 cm ×25 cm, grid size 1.25 cm^2) and video recorded. The number of errors (mice misplacing their forelimbs and falling off the grid) was recorded out of a total of 100 steps of the forelimbs of the mice.

Rotarod

The rotarod test was performed to assess post-stroke motor deficits as previously described.[29] Mice were placed on a 3.0-cm-diameter rotarod (Zhongshi Technology, China) and trained to stay on the rotating rod for 300 s at a rate of 5 to 40 revolutions per minute.

Y maze

Spatial memory and cognitive function were assessed using the Y maze (three equal-length arms connected in the Y shape, with arms labeled A, B, and C, respectively.[30] To ensure that the experimental environment was quiet and standard light, the mice were placed in the center and free to explore for 8 min to adapt to the environment. When the experiment officially began, the mice were again placed in the center and the order in which the mice entered each arm was recorded. Consecutively entering three arms (e.g., ABC, ACB, CAB, etc.) was defined as spontaneous alternation. The evaluation index was the percentage of spontaneous alternations (%), equal to the number of alternations/(total number of entries to each arm−2) × 100%.

Object location recognition test

Object Location Recognition was carried on as reported by Wang et al.[31] Mice were first acclimatized for half an hour and then another 10 min after two identical cubes were placed. The test began by changing the position of one object, allowing the mice to explore freely for 5 min, and recording the mice's exploratory behaviors towards moving objects, such as sniffing and biting, except for sitting on the object or randomly touching the object. The evaluation index is the percentage of the total detection time spent detecting the new location of the target.

Primary oligodendrocyte precursor cells (OPCs) culture

Primary OPCs were extracted using neonatal mice (P0-1) according to reference.[32] The cerebral cortex was isolated and PDGFRα$^+$ cells were enriched with CD140 (PDGFRα) MicroBead Kit (130-101-502, Meltenyi, USA). Primary OPCs were then cultured in a petri dish coated with poly-dimethylornithine (P0421, Sigma, USA) with the culture medium including DMEM/F12 (11320-033, Gibco, USA), 2% B27 (17504044, Invitrogen, USA), 20 ng/mL PDGF-AA (100-13 A, PeproTech, USA), 20 ng/mL bFGF (100-18B, PeproTech, USA). OPCs differentiation was induced by 50 ng/mL T3 (thyroid hormone) (T6397, Sigma, USA). The medium was replaced every 2 days for fresh medium. Staining with the OPCs marker PDGFRα showed that primary OPCs were successfully isolated (Figure S3(B)).

Oxygen-glucose deprivation/reoxygenation (OGD/R)-induced ischemia in vitro

The OGD/R model was used to simulate the ischemia as described previously.[33] In brief, after being replaced with glucose-free DMEM medium (L160KJ, BasalMedia, China), the cells were placed in a hypoxia incubator (Thermo Scientific, Marietta, OH) for 2 h at 37°C with 5% CO_2/95% N_2. The cells were then continued to be cultured in the normal medium under normoxic conditions with 5% CO_2/95% air.

OPCs proliferation assay

Cell counting kit-8 (CCK-8)

A cell counting kit (K1018, APExBIO, USA) was used to detect the viability of OPCs, according to the instructions. The OPCs (with a density of 1×10^4 per well) were inoculated on 96 wells of PDL coating, cultured with proliferation medium for 1–2 days, then treated with DPSCs-Exos or an equal volume PBS for 0–72 h, and treated with CCK8 at different time points.

EdU assay

According to the instruction manual of EdU (C0071S, Beyotime, China), dilute the EdU stock solution to 10 μM with OPCs medium, add cells and continue to incubate the cells for 3 h. After removing the medium, the cells were washed with PBS, then stabilized by 4% PFA at room temperature, and added to a permeabilized solution consisting of PBS and TritonX-100. PBS washed the cells, and the reaction solution was configured according to the kit instructions, then incubated with the cells in the dark. After final washing as well as nuclear staining, EdU-labeled and unlabeled cells were observed using a fluorescence microscope.

Injection and staining of EdU

In brief, the thymidine analog EdU (C00054, Ribobio, China, 50 mg/kg) was intraperitoneally injected into mice on day 3 after MCAO, once a day for 5 days. The Click reaction was performed according to the reagent instructions. Then anti-CC1 antibody (ab16794, Abcam, UK) was incubated overnight in a 4°C shaker, and Cyanine3 goat anti-mouse IgG (A10521, Invitrogen, USA) was then incubated for 2 h at room temperature.

Transmission electron microscopy

Mice were perfused transcardially with 4% PFA and fixed with 2.5% glutaraldehyde (4 °C, 4 h), then rinsed with PBS buffer (0.1 M). Samples were fixed using 1% starvation acid for 2 h, dehydrated, and permeabilized for more than 48 h. Ultrathin sections were then performed using the ultramicrotome (Leica, EM UC7) with a thickness of 70 nm. Final staining with lead citrate was performed for visualization using Leica TEM. The g-ratio of about 100 axons in each group was analyzed by the ImageJ software as a quantitative method.

RNA isolation and quantitative real-time PCR (qRT-PCR)

Non-ischemic and ischemic hemispheric brain tissues after MCAO were fragmented by tissue grinder into a mixed suspension, and the total RNA in tissues was extracted according to the instructions of TRIzol Reagent Total RNA Isolation Kit (15596026CN, Invitrogen, USA), with determined concentration and stored at −80℃. All primers required for the determination of mRNA abundance of target genes were purchased from Tsingke Biotech (Beijing, China. The qPCR experiments were performed according to the ChamQ SYBR qPCR Master Mix (Vazyme, Q341-02, China) reagent instruction manual. ΔΔCt was used to calculate the relative quantification of mRNA, as previously described,[34] and expressed as 2-ΔΔCt values. The primer sequences were listed in Table S1.

Immunostaining

Sections were treated at room temperature with 5% BSA (Solarbio, A8010, China) for 2 h.[35] The brand and dilution ratio of primary antibodies were as follows: rabbit PDGFR-α (1:100; CST), mouse CC1 (1:100; Abcam, UK), rabbit NG2 (1:200; Millipore), rabbit MBP (1:200; CST), mouse SMI32 (1:200; Millipore), GFAP (1:500, Millipore), rabbit

NeuN (1:200; CST), mouse Iba-1 (1:200; Millipore), rabbit MAP2 (1:400; Abcam), goat CD31 (1:200; RD), rabbit PRMT5 (1:200, CST), rabbit ID2 (1:200, CST). The incubation conditions for primary and secondary antibodies were 4°C overnight and 2 h away from light at room temperature, respectively. The nucleus was labeled with 4, 6-diamidino-2-phenylindole (DAPI, 1:600, Sigma, USA). The antibodies were listed in Table S2.

Western blot analysis

The protein concentration of the sample was determined and analyzed by BCA protein detection kit (P0009, Beyotime, China).[36] The total protein (30μg) after the addition of protein loading buffer was denatured at high temperature and subjected to gel electrophoresis with 10%–12% SDS-PAGE. The proteins in the gel were transferred by electro-transferring to the solid phase PVDF membrane (Millipore, USA), then blocked for 2 h at room temperature with the addition of 5% skimmed milk configured in TBST (0.1% Tween-20 included in Tris-buffered saline). Added diluted primary antibodies according to different experimental purposes and incubated overnight at 4°C. The next day, the relevant secondary antibody according to the species of primary antibody was added and incubated for 1 h at room temperature. The transferred proteins were treated with an enhanced Chemiluminescence substrate (34580, Thermofisher, USA) and the PVDF membrane was exposed to the Chemiluminescence imaging system (5200, Tanon, China). The antibodies were listed in Table S2.

Immunoprecipitation (IP)-MS

IP was performed as previously described by Zhan et al.[37] OPCs under different treatments were washed with PBS, followed by the addition of Immunoprecipitation lysis buffer (Beyotime, P0013, China) containing protease inhibitor (Roche, Cat. 4693132001), which was lysed for at least 30 min at 4°C. Transferred the lysate suspension and centrifuged it for 30 min at 12,000*g* at 4°C, transferred the liquid supernatant, and added PRMT5 Antibody (79998S, CST, USA), spinner-incubated for 12 h at 4°C. Protein A agarose beads (P2053, Beyotime, China) were added to the protein-antibody complexes with continued low-temperature spinning incubation for 3 h. The mobile phase A and B were disigned as 0.1% formic acid aqueous and 0.1% formic acetonitrile aqueous solution, respectively, and a C18 silica gel capillary column (3 μm, 120 Å, 100 mm × 150 mm) was selected to separate the peptides, and the flow rate was limited to 300 mL/min. The acquisition mode was data-dependent, starting with one full MS1 scan (range (m/z), 300–1600) followed by 20 MS2 scans. The data were retrieved from the UniProt database and analyzed using Proteome Discoverer 1.4 software.

Lentiviral vector transduction

Lentiviral vector transduction as previously described by Li et al.[8] OPCs were transduced with HBLV-m-PRMT5 shRNA-ZsGreen-PURO, control empty shRNA lentivirus, HBLV-m-ID2-3xflag- ZsGreen-PURO, and overexpression control lentivirus (Hanbio Tech, Shanghai, China) at MOI of 40 for 48 h in a cell culture incubator according to the company's instructions. The GFP signal was further observed under a fluorescence microscope to ensure the transduction efficiency.

Transfection

Mouse Myl9 siRNA (GAACCCCACAGACGAGUAUTT) and NC siRNA (UUCUCCGAACGUGUCACGUTT) were synthesized by Genepharm (Shanghai, China) and stored at −80°C. Transfection of the Myl9-siRNA (60 nM) and NC-siRNA (60 nM) into OPCs at 60% confluency in six-well plates was performed using JetPrime transfection reagent (101000046, Polyplus, French). The mouse-derived or human-derived CDS region of Myl9 was constructed into pcDNA3.1 (flag). Store the recombinant vector at −80°C. Transfection of the mouse-derived or human-derived Myl9 and pcDNA3.1 (+) into OPCs at 60% confluency in six-well plates was performed using JetPrime transfection reagent.

Statistical analysis

The mean ± SD was used to calculate the data of all experiments. One-way or two-way ANOVA was performed using IBM SPSS statistics 25. Differences were analyzed using Newman-Keuls post hoc or Bonferroni post hoc tests to compare statistical results. When $p < 0.05$, the differences were defined as statistically significant. All statistical programs in the experiment were demonstrated using GraphPad Prism software version 5.0 (La Jolla, CA, USA).

Results

DPSCs-Exos promoted neurological recovery after ischemic stroke

DPSCs-Exos were injected into the lateral ventricle on days 1, 3, and 5 of reperfusion, and morphological and behavioral tests were performed on 3, 7, and 14 days (Figure 1(a)). Cellular uptake of DPSCs-Exos in the brain showed that DPSCs-Exos could be taken up by OPCs (Figure 1(b)). Neurobehavioral and cognitive function tests were performed within 14 days after the MCAO model. Compared with the PBS group, the DPSCs-Exos group showed decreased neurological scores (Figure 1(c)), reduced number of right turns in the corner test (Figure 1(c)) and missteps in the foot fault test (Figure 1(d)), and increased latency to fall in the rotarod test (Figure 1(d)). In

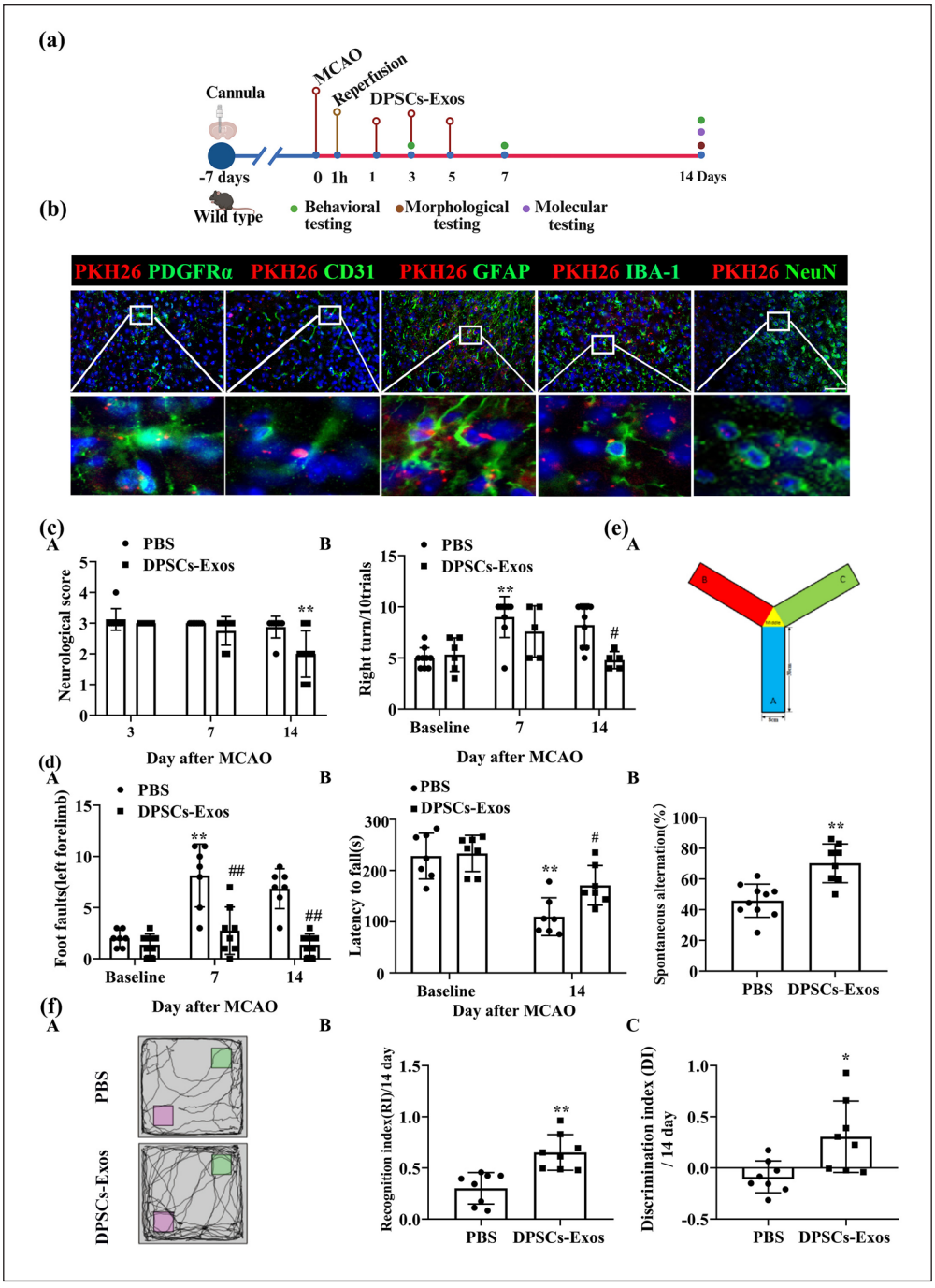

Figure 1. DPSCs-Exos delivery promotes recovery of sensorimotor and cognitive function after ischemic stroke in mice. (a) Schematic timeline of the experimental procedure. (b) Uptake of PKH26-labeled DPSCs-Exos by microglia, endothelial cells, astrocytes, OPCs, and neurons (Scale bar = 50 μm). (c) Neurologic scores (c, A), corner test (c, B), (d) foot-fault experiment (d, A), and rotarod (d, B) showed that DPSCs-Exos treatment promoted the sensory-motor function on 3, 7, and 14 days (d) after MCAO in mice (**$p < 0.01$ vs the baseline, #$p < 0.05$ ##$p < 0.05$ vs the PBS group, $n = 7$–9/group). (e) Y maze analysis shows that DPSCs-Exos treatment promoted the working memory in mice on 14 days after MCAO. (e, A) Schematic diagram of the Y maze. (e, B) Free alternation rate analysis in the PBS and DPSCs-Exos groups (**$p < 0.01$ vs the PBS group, $n = 9$/group). (f) The recognition index (B) and discrimination index (C) showed that DPSCs-Exos treatment promoted the recognition memory on 14 days after MCAO using object position recognition (*$p < 0.05$ vs the PBS group, $n = 8$/group).

addition, DPSCs-Exos treatment improved working memory in the Y-maze (Figure 1(e)), recognition memory in the novel object location test (Figure 1(f)), and significantly alleviated I/R-induced spatial learning and memory in the Morris water maze test (Figure S2(A)–(D)).

DPSCs-Exos treatment facilitated OPCs differentiation and white matter integrity repair after ischemic stroke

DPSCs-Exos treatment significantly alleviated ischemic stroke-induced white matter injury as shown by decreased myelin basic protein (MBP) and increased the expression of SMI32, a marker of white matter injury[38] in the cortex (CTX), external capsule (EC), and striatum (STR) in the ischemic hemisphere (I) of the brain 14 days after cerebral ischemia (Figure 2(a)). Western blot results confirmed the effect of DPSCs-Exos on decreased expression of MBP (Figure 2(b)). In addition, transmission electron microscopy (TEM) examination showed that DPSCs-Exos was able to promote the expression of myelinated axons after ischemia, as well as a decrease in the G ratio (Figure 2(c)). Ranvier nodes by immunostaining for Caspr1 and Nav1.6 markers.[5] In PBS-treated mice, Ranvier nodes were decreased, but DPSCs-Exos transplantation increased the number of Ranvier nodes (Figure 2(d)). Immunostaining showed that DPSCs-Exos treatment ameliorated the impaired OPCs differentiation (PDGFRα) and facilitated the generation of OLs (CC1) at 14 days after ischemia (Figure 2(e) and (f)). The effect of DPSCs-Exos on the proliferation and differentiation of OPCs was explored in vitro (Figure S3(A)). DPSCs-Exos increased OPCs proliferation and differentiation (Figures S3(D)–(F) and S4(A)–(C)). Primary OPCs were subjected to oxygen-glucose deprivation/reoxygenation (OGD/R) and then treated with DPSCs-Exos, indicating that DPSCs-Exos can promote the proliferation and differentiation of OPCs after OGD/R (Figure S4(D)–(F)).

DPSCs-Exos initiated OPCs differentiation and white matter repair by regulating PRMT5/ID2 after ischemic stroke

ID2 is a negative transcription factor regulating oligodendroglial differentiation.[16] Therefore, we checked the effect of DPSC-Exos on ID2. DPSCs-Exos treatment reduced the mRNA and protein levels of ID2 in primary OPCs (Figure 3(a) and (b)) and reduced ID2 mRNA expression in the ischemic hemisphere (Figure 3(b) and Figure S5(A)). DPSCs-Exos treatment was able to reduce the ischemia-induced ID2 elevation in oligodendrocytes (Figure 3(c)) and alleviated OGD/R-induced ID2 upregulation (Figure S5(H) and (J)). Overexpression of ID2 with lentiviral vectors was able to prevent the differentiation of OPCs (Figure 3(c)), but did not affect the OPCs proliferation (Figure S5(D) and (E)).

Knocking down PRMT5 in OPCs could reduce the differentiation of OPCs detected by MBP staining (Figure 3(d)) as well as reduce the proliferation of OPCs detected by EdU staining (Figure S5(F) and (G)). DPSCs-Exos treatment significantly increased PRMT5 protein expression in the OPCs nucleus, and the results were further confirmed by nucleoplasmic isolation experiments (Figure 3(e)). DPSCs-Exos treatment significantly alleviated OGD/R-induced PRMT5 decrease (Figure 3(f) and Figure S5(H) and (I)). DPSCs-Exos treatment was able to increase the expression level of PRMT5 protein in oligodendroglial profiles during recovery after ischemic stroke (Figure 3(g)). qPCR showed that there was no difference in the expression level of PRMT5 mRNA on the I hemisphere compared with the NI hemisphere (Figure S5(B)) and no difference in the expression of PRMT5 mRNA levels after DPSCs-Exos treatment compared with the PBS group (Figure S5(C)).

OPCs-specific knockdown of PRMT5 impedes white matter integrity and neurological recovery after ischemia in mice

OPCs-specific knockdown of PRMT5 ($PRMT5^{iOPCKO}$) hinders the neural functional recovery as shown by increased neurological functional scores, increased number of right turns in the corner experiment, decreased latency to fall in the rotarod experiment, and increased the number of missed steps in the foot fault experiment (Figure 4(a)–(c)). The memory was also impaired as shown by working memory impairment in the Y maze, recognition memory deficit in the object location recognition task 14 days after cerebral ischemia (Figure 4(d)–(f)). OPCs-specific knockdown of PRMT5 exacerbated postischemic brain injury as shown by MAP2 staining (Figure 5(a)). On day 28, obvious atrophy in the $PRMT5^{iOPCKO}$ mice could be seen in the gross photographs of whole brains (Figure 5(b)). OPCs-specific knockdown of PRMT5 aggravated white matter injury as shown by reduced number of Ranvier nodes (Figure 5(c)), decreased MBP expression and increased SMI32 expression after cerebral ischemia (Figure 5(d)), and impeded OPCs differentiation as shown by staining of PDGFRα and CC1 (Figure 5(e) and (f)). The specific knockdown of PRMT5 by OPCs increased the expression of ID2 in the OPCs (Figure 5(f)).

Myl9 from DPSCs-Exos regulated PRMT5 nucleoplasmic distribution in OPCs

Immunoprecipitation (IP) and mass spectrometry were performed to characterize the proteins in the DPSCs-Exos-treated OPCs that were able to promote PRMT5 entry into

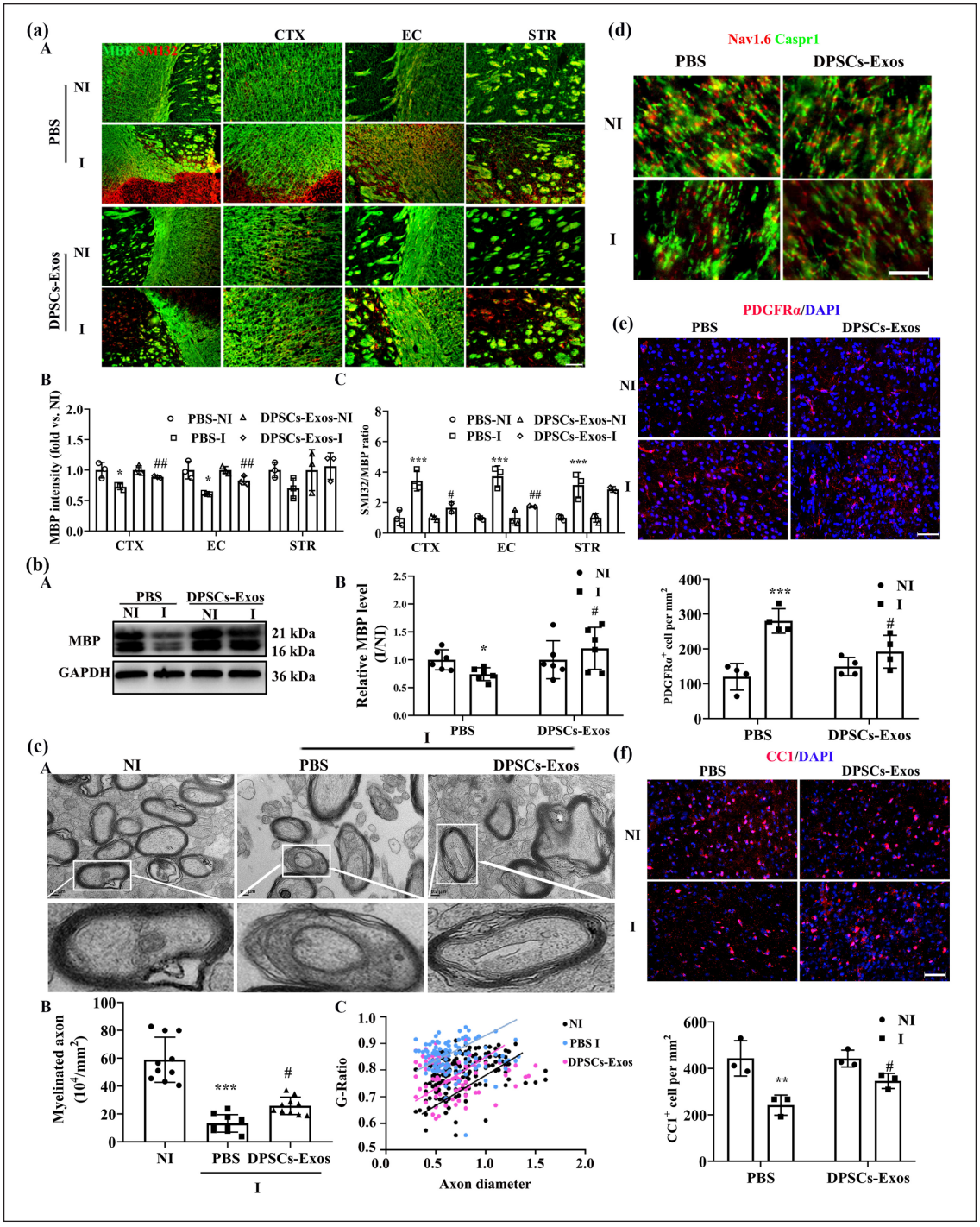

Figure 2. DPSCs-Exos treatment enhances OPCs differentiation and improves white matter integrity in mice 14 days after ischemic stroke. (a) Representative images of MBP and SMI32-positive staining (a, A) and quantification of MBP (a, B) and SMI32/MBP intensity (a, C) showed that DPSCs-Exos treatment significantly increased MBP and decreased SMI32 expression ($n = 3$/group, scale bar = 100 μm). (b) Representative western blot images (b, A) and quantification (b, B) showed that DPSCs-Exos treatment significantly inhibited ischemic stroke-induced MBP decrease ($n = 6$/group). (c) Representative transmission electron microscopy images (A) and quantification of the ratio of myelinated axons in the striatum (B, C) showed that DPSCs-Exos treatment significantly promoted myelin formation (Scale bar = 100 nm). (d) Nav1.6 and Caspr1 double-staining showed that DPSCs-Exos treatment significantly increased the number of Ranvier nodes (Scale bar = 5 μm). (e, f) Representative images and quantification of PDGFRα-positive OPCs (e) and CC1-positive mature oligodendrocytes (f) in the peri-infarction area showed that DPSCs-Exos-treatment significantly promoted OPCs differentiation.

NI: nonischemic; I: ischemic.

*$p < 0.05$, **$p < 0.01$, ***$p < 0.001$ vs the NI, #$p < 0.05$, ##$p < 0.01$ vs the PBS group, $n = 3$–4/group, scale bar = 50 μm.

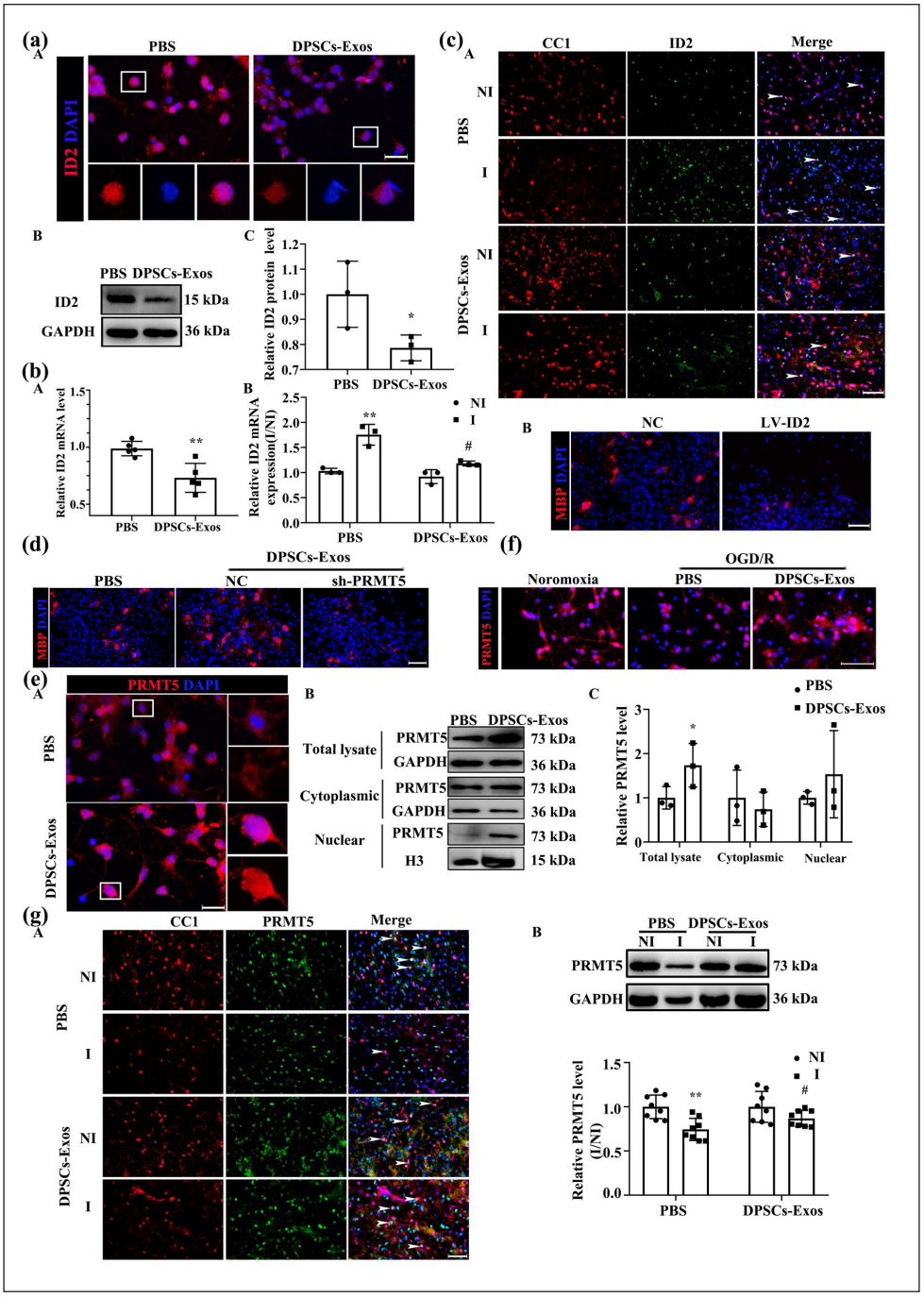

Figure 3. DPSCs-Exos treatment alleviates I/R-induced ID2 increase and PRMT5 decrease after cerebral ischemia. (a) ID2 immunostaining (a, A), representative immunoblots image, and quantification of ID2 protein (a (B, C)) showed that DPSCs-Exos treatment reduced ID2 expression (*$p < 0.05$ vs the PBS group, $n = 3$/group, scale bar = 20 μm). (b) Quantification of ID2 mRNA levels in vitro (b, A) and in vivo (b, B) showed that DPSCs-Exos treatment reduced *ID2* gene expression (**$p < 0.01$ vs NI, #$p < 0.05$ vs the PBS group, $n = 3$–5/group). (c, A) Representative images of ID2/CC1 immunostaining 14 days after MCAO showed that DPSCs-Exos treatment reduced ID2 expression in oligodendrocytes ($n = 3$/group, scale bar = 50 μm). NI, nonischemic; I, ischemic; (c, B) representative images of MBP-positive cells showed that ID2 overexpression obstructed OPCs differentiation (scale bar = 50 μm). (d) Representative images of MBP-positive cells showed that sh-PRMT5 obstructed OPCs differentiation (scale bar = 50 μm). (e) Immunostaining of PRMT5 (e, A), representative immunoblots image (e, B), and quantification of PRMT5 protein (e, C) showed that DPSCs-Exos treatment promoted PRMT5 nuclear translocation during OPCs differentiation (*$p < 0.05$ vs the PBS group, $n = 3$/group, scale bar = 20 μm). (f) Representative immunostaining images showed that DPSCs-Exos treatment promoted PRMT5 nuclear translocation after OGD/R. (g) Representative images of PRMT5/CC1 immunostaining (g, A), representative immunoblots image and quantification of PRMT5 protein (g, B) showed that DPSCs-Exos treatment increased PRMT5 expression in oligodendrocytes 14 days after MCAO (**$p < 0.01$ vs the NI, #$p < 0.05$ vs the PBS group, $n = 3$–8/group, scale bar = 50 μm).

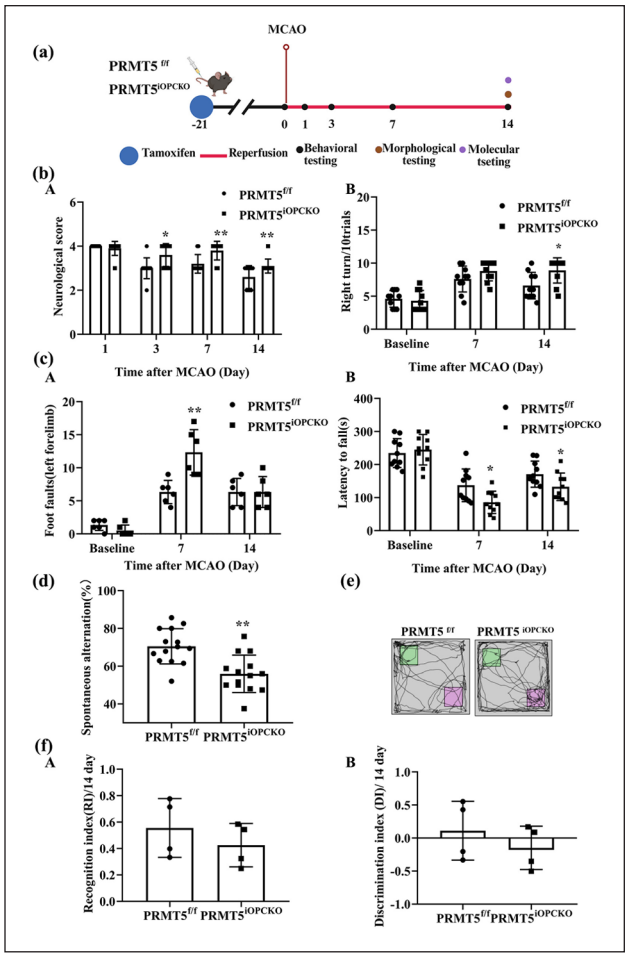

Figure 4. PRMT5 knockout exacerbates sensorimotor and cognitive deficits 14 days after ischemic stroke. (a) Schematic showing the experimental procedure timeline using PRMT5^{iOPCKO} mice. (b) Neurologic scores (b, A), corner test (b, B), (c) foot-fault experiment (c, A), and rotarod (c, B) showed that knockout PRMT5 in OPCs impaired sensory-motor function 7 and 14 days after ischemic stroke (*$p < 0.05$, **$p < 0.01$ vs the PRMT5$^{f/f}$ group, $n = 6$–10/group). (d) Y maze showed that knockout PRMT5 in OPCs impaired the working memory 14 days after ischemic stroke. (e) Schematic diagram of the object location recognition. (f) The recognition index (f, A) and discrimination index (f, B) in object location recognition showed that knockout PRMT5 in OPCs impaired the recognition memory 14 days after ischemic stroke ($n = 6$–10/group).

the nucleus (Figure 6(a)). Mass spectrometry results showed that a total of 351 proteins were identified that interacted specifically with PRMT5 after DPSCs-Exos treatment of OPCs (Figure S6(A)). Go analysis showed that the functional enrichment of the top 10 most divergent was mainly closely related to the myelin proteome (Figure S6(B)). This 351 cross-analysis with exosome mass spectrometry results yielded 29 identical proteins (Figure S6(C)). The following four proteins were selected by scoring as well as literature screening for Myl9, PPP2ca, Nup58, and NuP93 (Figure 6(b)). Myl9 is one of the factors that can promote myelin formation.[22] Overexpression of human-derived Myl9 in OPCs was able to promote PRMT5 entry into the nucleus (Figure 6(c) and (d) and Figure S6(D) and (E)), as well as proliferation and differentiation of OPCs (Figure 6(e) and (f)), while suppressing Myl9 could inhibit the OPCs differentiation (Figure 6(f)). These results suggest that Myl9 may directly target PRMT5 to promote oligodendrogliogenesis.

Discussion

Emerging evidence indicates a strong correlation between post-stroke white matter repair and neurological recovery.[4,5] While a substantial population of oligodendrocyte precursor cells (OPCs) resides in the peri-infarct region following ischemia,[39] only a small fraction differentiates into mature oligodendrocytes (OLs), limiting functional recovery.[6,8] Therefore, understanding the mechanism underlying OPCs differentiation and developing strategies to promote OPCs differentiation after ischemic stroke are crucial. Using a mouse model of middle cerebral artery occlusion (MCAO) and a cellular model of OGD/R, we investigated the impact of DPSCs-Exos on OPCs differentiation and white matter repair. Our key findings are: 1) DPSCs-Exos promote OPCs proliferation, differentiation, and white matter integrity; 2) mechanistically, DPSCs-Exos facilitate PRMT5 nuclear entry in OPCs, leading to altered methylation of CpG islands within the *ID2* gene, subsequently downregulating ID2 expression, and thus promoting OPCs differentiation; 3) PRMT5 knockout inhibits OPCs differentiation and white matter repair after ischemic stroke; 4) Myosin light chain 9 (Myl9) within DPSCs-Exos interacts with PRMT5 in OPCs, driving PRMT5 nuclear translocation. In conclusion, our results demonstrate that DPSCs-Exos promote OPCs differentiation and white matter repair via the Myl9/PRMT5/ID2 axis following ischemic stroke (Figure 7).

Dysfunction of OPCs differentiation and white matter repair are key pathological factors limiting neural function recovery after ischemic stroke.[40] Currently, no approved drugs or targeted therapies exist for these conditions. In the study, we show that DPSCs-Exos promote OPCs differentiation and white matter repair both in vitro and in vivo. In addition, DPSCs-Exos have been shown to inhibit neuroinflammation and microglial pyroptosis in subarachnoid hemorrhage,[41] and DPSCs-conditioned medium can alleviate subarachnoid hemorrhage-induced microcirculation impairment by promoting M2 microglia polarization and reducing astrocyte swelling.[42] Compared with stem cell transplantation, exosomes offer several advantages, including the ability to cross the BBB and simplified storage and transportation. These properties suggest that DPSCs-Exos hold significant promise for stimulating OPCs differentiation and white matter repair following ischemic stroke.

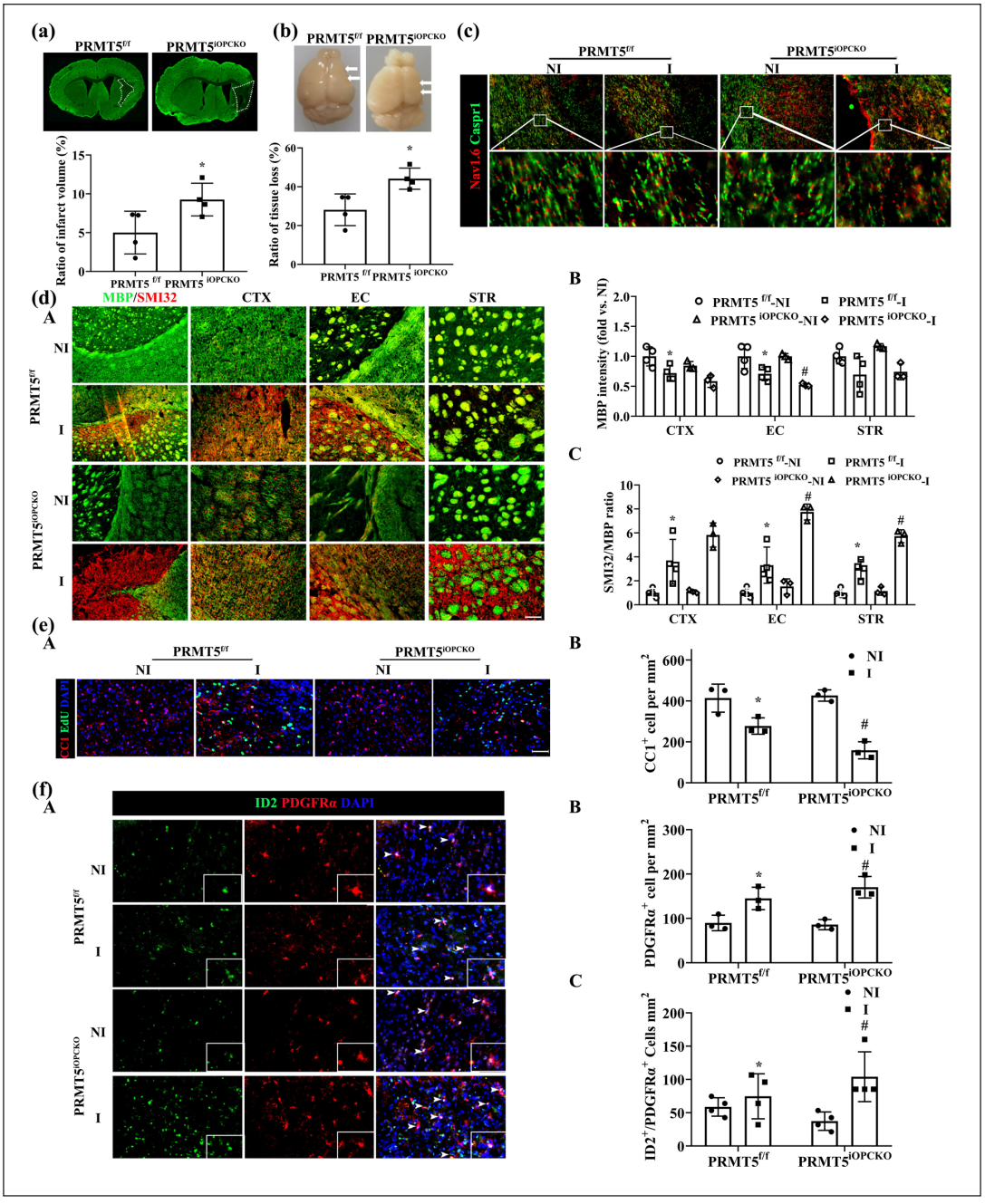

Figure 5. PRMT5 knockout impedes OPC differentiation and white matter integrity repair after ischemic stroke. (a) Representative MAP2 immunofluorescence and quantification of cerebral infarct volume 14 days after ischemia showed that knockout PRMT5 in OPCs aggravated cerebral infarction (*$p < 0.05$ vs PRMT5$^{f/f}$ mice, $n = 4$/group). (b) Photographs of whole brains 28 days and quantification of cerebral atrophy area after ischemia showed that knockout PRMT5 in OPCs aggravated cerebral atrophy. Arrows indicated lesion area and brain atrophy (*$p < 0.05$ vs PRMT5$^{f/f}$ mice, $n = 4$/group). (c) Representative Nav1.6 and Caspr1 double-staining showed that PRMT5^{iOPCKO} mice reduced the number of Ranvier nodes (Scale bar = 50 μm). (d) Representative MBP/SMI32 immunofluorescence (d, A) and quantitative analysis of MBP (d, B) and SMI32/MBP intensity (d, C) showed that PRMT5^{iOPCKO} mice aggravated the loss of MBP and aggravated SMI32-positive staining 14 days after ischemia (*$p < 0.05$ vs NI of PRMT5$^{f/f}$ mice, #$p < 0.05$ vs I of PRMT5^{iOPCKO} mice, $n = 3$–4/group, scale bar = 100 μm). (e) Representative images (e, A) and quantitative analysis of EdU and CC1 immunofluorescence in the peri-infarct lesions (e, B) showed that PRMT5^{iOPCKO} mice aggravated the loss of CC1$^+$ cells 14 days after ischemia (*$p < 0.05$ vs NI of PRMT5$^{f/f}$ mice, #$p < 0.05$ vs I of PRMT5^{iOPCKO} mice, $n = 3$/group, scale bar = 50 μm). (f) Representative images (f, A) and quantitative analysis of PDGFRα-positive cells (f, B) and PDGFRα/ID2 positive cells (f, C) in lesions showed that PRMT5^{iOPCKO} mice aggravated the increase in OPCs and promoted ID2 expression in OPCs at 14 days after MCAO (*$p < 0.05$, vs the NI, #$p < 0.05$ vs the I of PRMT5^{iOPCKO} mice, $n = 4$/group, scale bar = 50 μm).

NI: nonischemic; I: ischemic.

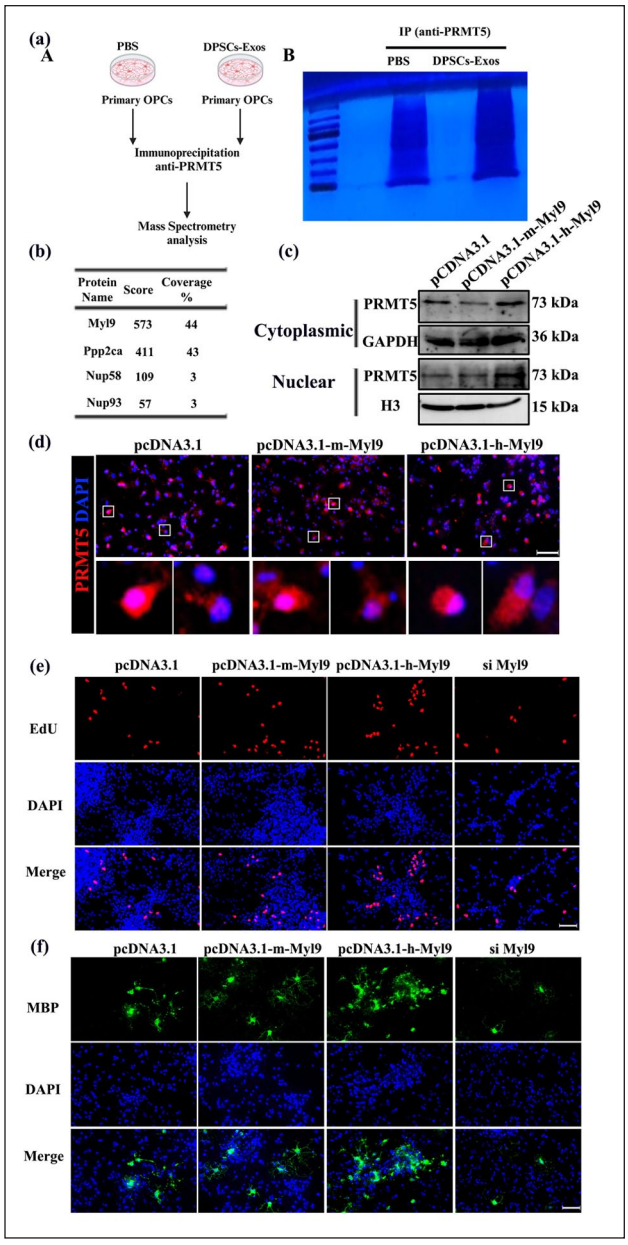

Figure 6. Myl9 from DPSCs-Exos regulates PRMT5 nucleoplasmic distribution in OPCs. (a) An illustration of the IP-MS strategies used for exploring endogenous PRMT5-binding proteins in DPSCs-Exos-treated OPCs (a, A), and Coomassie Blue staining showed the gel containing PRMT5 interactive proteins (a, B). (b) Identification of four proteins (i.e., Myl9, PPP2ca, Nup58, and NuP93) through MS scoring and literature search. (c) Representative immunoblots showed that overexpression of human-derived Myl9 promoted nuclear translocation of PRMT5 within OPCs. (d) Immunostaining of PRMT5 showed that overexpression of human-derived Myl9 promoted nuclear translocation of PRMT5 within OPCs ($n = 3$/group, scale bar = 50 μm). (e, f) Representative images of EdU-positive cells (e) and MBP-positive cells (f) showed that overexpression of human-derived Myl9 promoted OPCs proliferation and differentiation (scale bar = 50 μm).

Nuclear ID2 can negatively regulate the development and maturation of OLs.[13–16] Therefore, limiting ID2 within the cytoplasm or reducing its nuclear expression are potential strategies to promote OPCs differentiation. In this study, we demonstrate that treatment with DPSCs-Exos reduces ID2 expression in the nucleus, suggesting that DPSCs-Exos may be an effective means of achieving this goal. In addition, PRMT5 plays an important role in OPCs differentiation[20,43] and AS-2P, a stable form of vitamin C, can attenuate chronic hypoxia-induced white matter injury by regulating PRMT5.[44] In this study, we demonstrate that PRMT5 knockout hinders spontaneous neural functional recovery, white matter repair, and OPCs differentiation, and treatment with DPSCs-Exos increases PRMT5 expression and promotes its entry into the nucleus. Furthermore, Consistent with previous research that PRMT5 binds to CpG-rich islands within the *ID2* gene to play a role in gene silencing during OPCs differentiation,[19] here, we show that DPSCs-Exos decrease nuclear *ID2* expression by regulating PRMT5.

In the present study, we demonstrate that DPSCs-Exos promote the nuclear localization of PRMT5 in OPCs. Specifically, DPSCs-Exos containing Myl9 interact with PRMT5 to promote OPCs differentiation by facilitating PRMT5 nuclear entry. Furthermore, overexpression of Myl9 also induces PRMT5 nuclear translocation and OPCs differentiation. These findings suggest that Myl9 within DPSCs-Exos is crucial for the therapeutic effects observed in promoting oligodendrogenesis and white matter repair.

While in this study, we demonstrate the potential of DPSCs-Exos to promote OPCs differentiation and white matter integrity restoration after ischemic stroke, likely through direct action on OPCs, we cannot rule out the possibility of DPSCs-Exos also influencing other cell types. Our investigation into DPSCs-Exos uptake across various cell types, including microglia, astrocytes, endothelial cells, and neurons, confirms that DPSCs-Exos are indeed taken up by cells beyond OPCs. This suggests that the therapeutic effects of DPSCs-Exos in ischemic stroke may extend beyond their impact on OPCs and involve the contributions of other cell types as well. In addition, there are limitations in labeling exosomes with PKH26, which, due to its lipophilicity, carries the risk of transfer to other cells and lipids when labeling exosomes. This transfer can result in false positives and high background noise, leading to erroneous conclusions about exosome biodistribution, uptake capacity, and functional studies. Therefore, the use of PKH26 is dependent on precise ultracentrifugation cleaning and optimized labeling conditions. Although it cannot be eliminated, the risk of transfer can be minimized through a strict experimental design.

In conclusion, our findings in the present study reveal that DPSCs-derived exosomes promote OPCs differentiation and

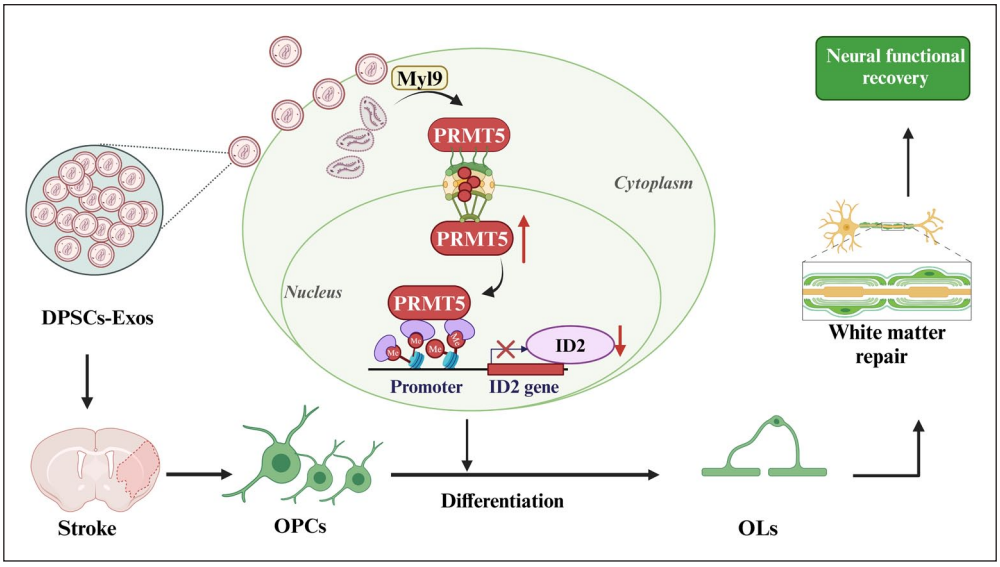

Figure 7. A schema showing the proposed molecular mechanism that DPSCs-Exos improves neurological recovery after ischemic stroke by promoting the entry of PRMT5 into the nucleus of OPCs through Myl9, down-regulating the expression of ID2, and promoting the differentiation of OPCs, the repair of white matter integrity.

white matter repair following ischemic stroke. Mechanistically, this is achieved through the facilitation of PRMT5 nuclear entry in OPCs, leading to Myl9-mediated downregulation of *ID2* expression.

Author contributions

X.J. conceived the concept, designed the research, interpreted data, and wrote the manuscript. C.G. wrote the manuscript. W.D., P.G., Z.L., Y.S., Y.Z. conducted the research and/or analyzed data

Funding

The authors disclosed receipt of the following financial support for the research, authorship, and/or publication of this article: This work was also supported by National Key R&D Program of China (2022YFC3602805), by the Scientific Research Common Program of Beijing Municipal Commission of Education (KM202310025027), by Beijing Natural Science Foundation (7252192). This work was also supported by the National Natural Science Foundation of China (81870973, 82574397).

Declaration of conflicting interests

The authors declared the following potential conflicts of interest with respect to the research, authorship, and/or publication of this article: X.J., W.D., and P.G. are inventors on a patent application related to this work filed to the National Intellectual Property Administration, the People's Republic of China (No. 202411612051. X; filed 13 November 2024). The other authors declare that they have no competing interests.

ORCID iDs

Chun Guo https://orcid.org/0000-0002-1540-3166
Xinchun Jin https://orcid.org/0000-0002-5351-7914

Supplemental material

Supplemental material for this article is available online.

References

1. Pantoni L, Garcia JH and Gutierrez JA. Cerebral white matter is highly vulnerable to ischemia. *Stroke* 1996; 27(9): 1641–1646; discussion 1647.
2. Wang Y, Liu G, Hong D, et al. White matter injury in ischemic stroke. *Prog Neurobiol* 2016; 141: 45–60.
3. Etherton MR, Wu O, Giese AK, et al. White matter integrity and early outcomes after acute ischemic stroke. *Transl Stroke Res* 2019; 10(6): 630–638.
4. Jia J, Xu S, Hu J, et al. Growth arrest specific protein 6 alleviated white matter injury after experimental ischemic stroke. *J Cereb Blood Flow Metab* 2024; 44(1): 77–93.
5. Zhang W, Pu H, Hu X, et al. Poststroke intravenous transplantation of human mesenchymal stem cells improves brain repair dynamics and functional outcomes in aged mice. *Stroke* 2023; 54(4): 1088–1098.
6. Li F, Liu WC, Wang Q, et al. NG2-glia cell proliferation and differentiation by glial growth factor 2 (GGF2), a strategy to promote functional recovery after ischemic stroke. *Biochem Pharmacol* 2020; 171: 113720.
7. Cheng YJ, Wang F, Feng J, et al. Prolonged myelin deficits contribute to neuron loss and functional impairments after ischaemic stroke. *Brain* 2024; 147(4): 1294–1311.
8. Li Y, Liu Z, Song Y, et al. M2 microglia-derived extracellular vesicles promote white matter repair and functional recovery via miR-23a-5p after cerebral ischemia in mice. *Theranostics* 2022; 12(7): 3553–3573.
9. Gong P, Tian Q, He Y, et al. Dental pulp stem cell transplantation facilitates neuronal neuroprotection following cerebral ischemic stroke. *Biomed Pharmacother* 2022; 152: 113234.

10. Grawish ME. Human dental pulp stem/stromal cells in clinical practice. *World J Stem Cells* 2024; 16(2): 54–57.
11. Nito C, Suda S, Nitahara-Kasahara Y, et al. Dental-pulp stem cells as a therapeutic strategy for ischemic stroke. *Biomedicines* 2022; 10(4): 737.
12. Du W, He Y, Li L, et al. The effects and mechanisms of stem cells and exosomes on neurological function protection and recovery after ischemic stroke. *Neuroprotection* 2025; 3: 266–279.
13. Tiane A, Schepers M, Riemens R, et al. DNA methylation regulates the expression of the negative transcriptional regulators ID2 and ID4 during OPC differentiation. *Cell Mol Life Sci* 2021; 78(19–20): 6631–6644.
14. Wang Y, Jiang A, Yan J, et al. Inhibition of GPR17/ID2 axis improve remyelination and cognitive recovery after SAH by mediating OPC differentiation in rat model. *Transl Stroke Res* 2025; 16(2): 178–193.
15. Boccazzi M, Macchiarulo G, Lebon S, et al. G protein-coupled receptor 17 is regulated by WNT pathway during oligodendrocyte precursor cell differentiation. *Neurobiol Dis* 2023; 187: 106315.
16. Chen XS, Zhang YH, Cai QY, et al. ID2: a negative transcription factor regulating oligodendroglia differentiation. *J Neurosci Res* 2012; 90(5): 925–932.
17. Wang S, Sdrulla A, Johnson JE, et al. A role for the helix-loop-helix protein Id2 in the control of oligodendrocyte development. *Neuron* 2001; 29(3): 603–614.
18. Lasorella A and Iavarone A. The protein ENH is a cytoplasmic sequestration factor for Id2 in normal and tumor cells from the nervous system. *Proc Natl Acad Sci U S A* 2006; 103(13): 4976–4981.
19. Huang J, Vogel G, Yu Z, et al. Type II arginine methyltransferase PRMT5 regulates gene expression of inhibitors of differentiation/DNA binding Id2 and Id4 during glial cell differentiation. *J Biol Chem* 2011; 286(52): 44424–44432.
20. Scaglione A, Patzig J, Liang J, et al. PRMT5-mediated regulation of developmental myelination. *Nat Commun* 2018; 9(1): 2840.
21. Dansu DK, Liang J, Selcen I, et al. PRMT5 interacting partners and substrates in oligodendrocyte lineage cells. *Front Cell Neurosci* 2022; 16: 820226.
22. Sharma AD, Wiederin J, Uz M, et al. Proteomic analysis of mesenchymal to Schwann cell transdifferentiation. *J Proteomics* 2017; 165: 93–101.
23. Chen S, Sun Y, Li F, et al. Modulation of alpha7nAchR by melatonin alleviates ischemia and reperfusion-compromised integrity of blood-brain barrier through inhibiting hmgb1-mediated microglia activation and crtc1-mediated neuronal loss. *Cell Mol Neurobiol* 2022; 42(7): 2407–2422.
24. Kong F, Wu CT, Geng P, et al. Dental pulp stem cell-derived extracellular vesicles mitigate haematopoietic damage after radiation. *Stem Cell Rev Rep* 2021; 17(2): 318–331.
25. Zhang S, Thiebes AL, Kreimendahl F, et al. Extracellular vesicles-loaded fibrin gel supports rapid neovascularization for dental pulp regeneration. *Int J Mol Sci* 2020; 21(12): 4226.
26. Zhou K, Tan Y, Zhang G, et al. Loss of SARM1 ameliorates secondary thalamic neurodegeneration after cerebral infarction. *J Cereb Blood Flow Metab* 2024; 44(2): 224–238.
27. Ge Y, Dou X, Chen P, et al. Treadmill exercise enhances post-stroke functional recovery in mice via the CX3CL1/CX3CR1 signaling pathway. *Mol Neurobiol* 2025; 62(1): 591–603.
28. Liu Y, Liu WC, Sun Y, et al. Normobaric hyperoxia extends neuro- and vaso-Protection of N-acetylcysteine in transient focal ischemia. *Mol Neurobiol* 2017; 54(5): 3418–3427.
29. Mehta SL, Chelluboina B, Morris-Blanco KC, et al. Post-stroke brain can be protected by modulating the lncRNA FosDT. *J Cereb Blood Flow Metab* 2024; 44(2): 239–251.
30. Callaghan RM, Yang H, Moloney RD, et al. Behavioral assessment of neuropsychiatric outcomes in rodent stroke models. *J Cereb Blood Flow Metab* 2025; 45(7): 1232–1248.
31. Wang Y, Zhang X, Guo H, et al. Aging-induced episodic-like memory impairment could be alleviated by melatonin treatment via preserving blood-brain barrier integrity and upregulating CRTC1. *CNS Neurosci Ther* 2025; 31(4): e70412.
32. Shi XY, He YX, Ge MY, et al. Gastrodin promotes CNS myelinogenesis and alleviates demyelinating injury by activating the PI3K/AKT/mTOR signaling. *Acta Pharmacol Sin* 2025; 46(6): 1610–1623.
33. Hu X, Dong J, Geng P, et al. Nicotine treatment ameliorates blood-brain barrier damage after acute ischemic stroke by regulating endothelial scaffolding protein Pdlim5. *Transl Stroke Res* 2024; 15(3): 672–687.
34. Wang X, Wang Q, Song M, et al. Chronic but not acute nicotine treatment ameliorates acute inflammation-induced working memory impairment by increasing CRTC1 and HCN2 in adult male mice. *CNS Neurosci Ther* 2024; 30(2): e14627.
35. Wang Q, Wang MW, Sun YY, et al. Nicotine pretreatment alleviates MK-801-induced behavioral and cognitive deficits in mice by regulating Pdlim5/CRTC1 in the PFC. *Acta Pharmacol Sin* 2023; 44(4): 780–790.
36. Zhang XL, Du WH, Qian SX, et al. Glial growth factor 2 treatment alleviates ischemia and reperfusion-damaged integrity of the blood-brain barrier through decreasing Mfsd2a/caveolin-1-mediated transcellular and Pdlim5/YAP/TAZ-mediated paracellular permeability. *Acta Pharmacol Sin* 2024; 45(11): 2241–2252.
37. Zhan R, Meng X, Tian D, et al. NAD(+) rescues aging-induced blood-brain barrier damage via the CX43-PARP1 axis. *Neuron* 2023; 111(22): 3634.e7–3649.e7.
38. Mi Z, Povysheva N, Rose ME, et al. Abolishing UCHL1's hydrolase activity exacerbates ischemia-induced axonal injury and functional deficits in mice. *J Cereb Blood Flow Metab* 2024; 44(11): 1349–1361.
39. Hu X, Geng P, Zhao X, et al. The NG2-glia is a potential target to maintain the integrity of neurovascular unit after acute ischemic stroke. *Neurobiol Dis* 2023; 180: 106076.
40. Wang S, Li C, Kang X, et al. Agomelatine promotes differentiation of oligodendrocyte precursor cells and preserves white matter integrity after cerebral ischemic stroke. *J Cereb Blood Flow Metab* 2024; 44(12): 1487–1500.
41. Liang X, Miao Y, Tong X, et al. Dental pulp mesenchymal stem cell-derived exosomes inhibit neuroinflammation and

microglial pyroptosis in subarachnoid hemorrhage via the miRNA-197-3p/FOXO3 axis. *J Nanobiotechnology* 2024; 22(1): 426.

42. Yang LY, Chen YR, Lee JE, et al. Dental pulp stem cell-derived conditioned medium alleviates subarachnoid hemorrhage-induced microcirculation impairment by promoting M2 microglia polarization and reducing astrocyte swelling. *Transl Stroke Res* 2023; 14(5): 688–703.
43. Calabretta S, Vogel G, Yu Z, et al. Loss of PRMT5 promotes PDGFRalpha degradation during oligodendrocyte differentiation and myelination. *Dev Cell* 2018; 46(4): 426. e5–440.e5.
44. Ding B, Lou J, Qin T, et al. L-ascorbyl-2-phosphate alleviates white matter injury caused by chronic hypoxia through the PRMT5/P53/NF-kappaB pathway. *J Neurochem* 2024; 168(2): 142–160.